

## SUPPLEMENTARY INFORMATION

### Supramolecular Self-Assembly to Control Structural and Biological Properties of Multicomponent Hydrogels

Babatunde O. Okesola<sup>1,2</sup>, Yuanhao Wu<sup>1,2</sup>, Burak Derkus<sup>1,2,3</sup>, Sammar Gani<sup>4</sup>, Dong Sheng Wu<sup>2</sup>, Dafna Knani<sup>4</sup>, David K. Smith<sup>5</sup>, David J. Adams<sup>6</sup>, Alvaro Mata<sup>1,2\*</sup>

1. Institute of Bioengineering, Queen Mary University of London, London, E1 4NS, UK.
2. School of Engineering and Materials Science, Queen Mary University of London, London, E1 4NS, UK.
3. Biomedical Engineering Department, Faculty of Engineering, Eskisehir Osmangazi University, 26040 Eskisehir, Turkey.
4. Department of Biotechnology Engineering, ORT Braude College, P.O. Box 78, Karmiel 2161002, Israel.
5. Department of Chemistry, University of York, Heslington, York, YO10 5DD, UK.
6. School of Chemistry, University of Glasgow, Glasgow, G12 8QQ, UK.

\*Corresponding author: [a.mata@qmul.ac.uk](mailto:a.mata@qmul.ac.uk)

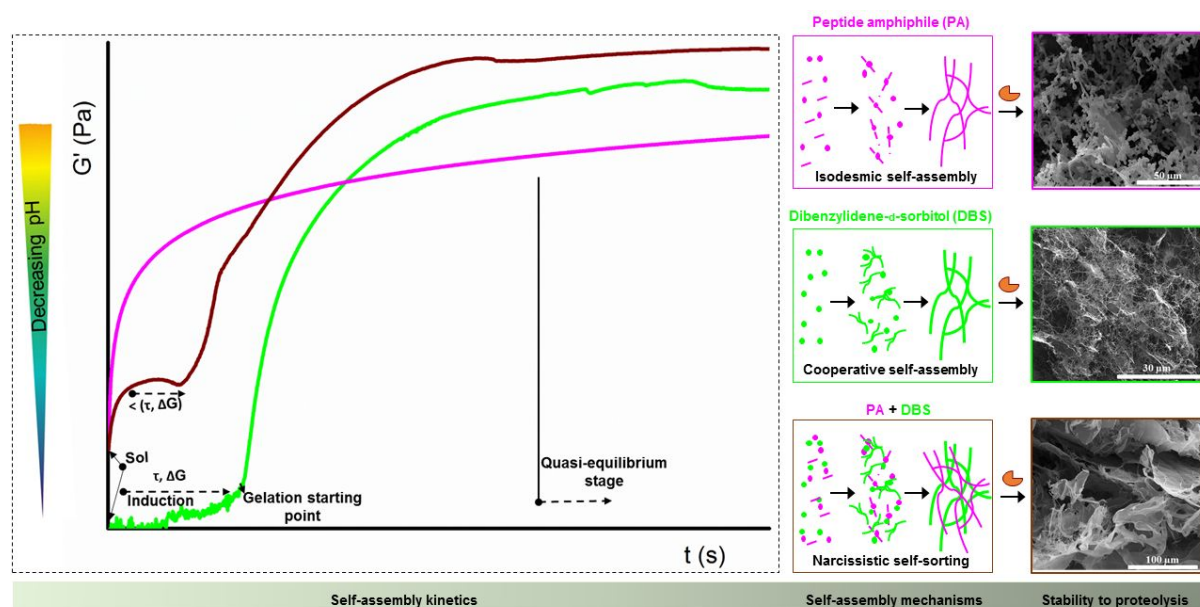
#### Contents

1. Synthesis
2. Overview of multicomponent self-assembly and benefits
3. ThT fluorescent microscopy assay
4. CD spectra for ThT interaction
5. TEM characterization of nanostructures of **PA-E3**, **DBS-COOH** and mixtures
6. Small-Angle Neutron Scattering (SANS) measurements
7. Rheological kinetics for **PA-E3**, **DBS-COOH** and **PA-E3/DBS-COOH** mixture
8. Avrami Equations
9. Molecular dynamics computation
10. Amplitude sweeps, critical strain and self-recovery of hydrogels
11. UV-TIC spectra for hydrogel digestion
12. References

## 1. Synthesis

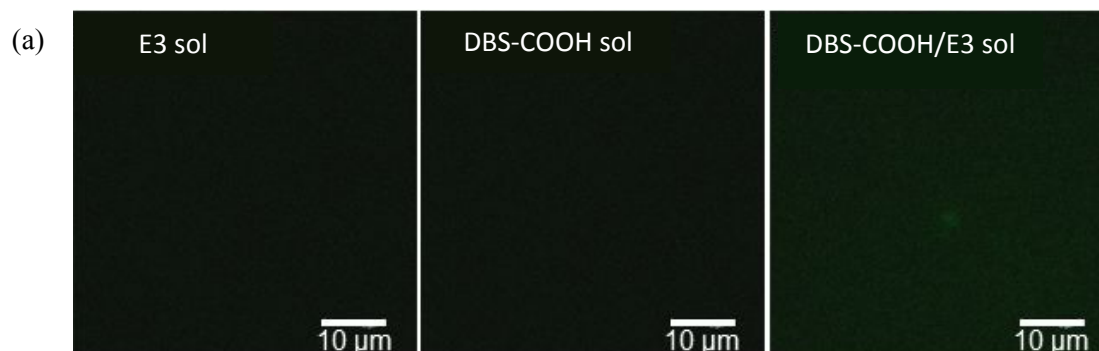
PA-E3 and DBS-COOH were synthesized and characterized as previously reported elsewhere.<sup>1,2</sup>

## 2. Overview of multicomponent self-assembly and benefits



**Figure S1.** Schematic representation of self-assembly kinetics, self-assembly mechanisms and response to proteolysis by peptide amphiphile (PA-E3), DBS-COOH and PA-E3/DBS-COOH.

## 3. Thioflavin T (Th T) fluorescence assay



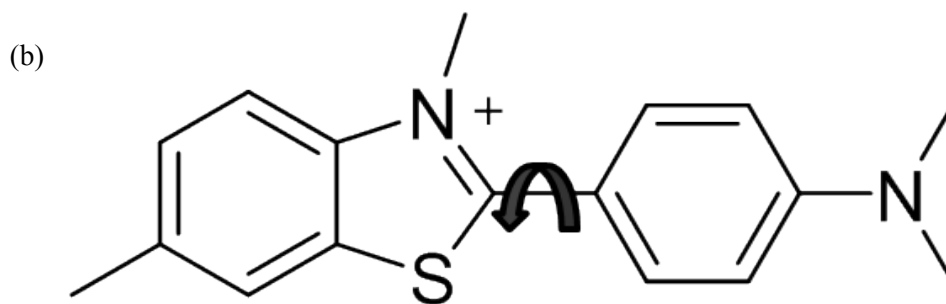


**Figure S2.** LSCM images of **PA-E3**, **DBS-COOH** and **DBS-COOH/PA-E3** sols showing that ThT showed a weak fluorescent signal in the sol state of the gelators. (b) Molecular structure of ThT showing the torsion angle between the benzothiazole and aminobenzene.

#### 4. CD measurement for ThT interactions

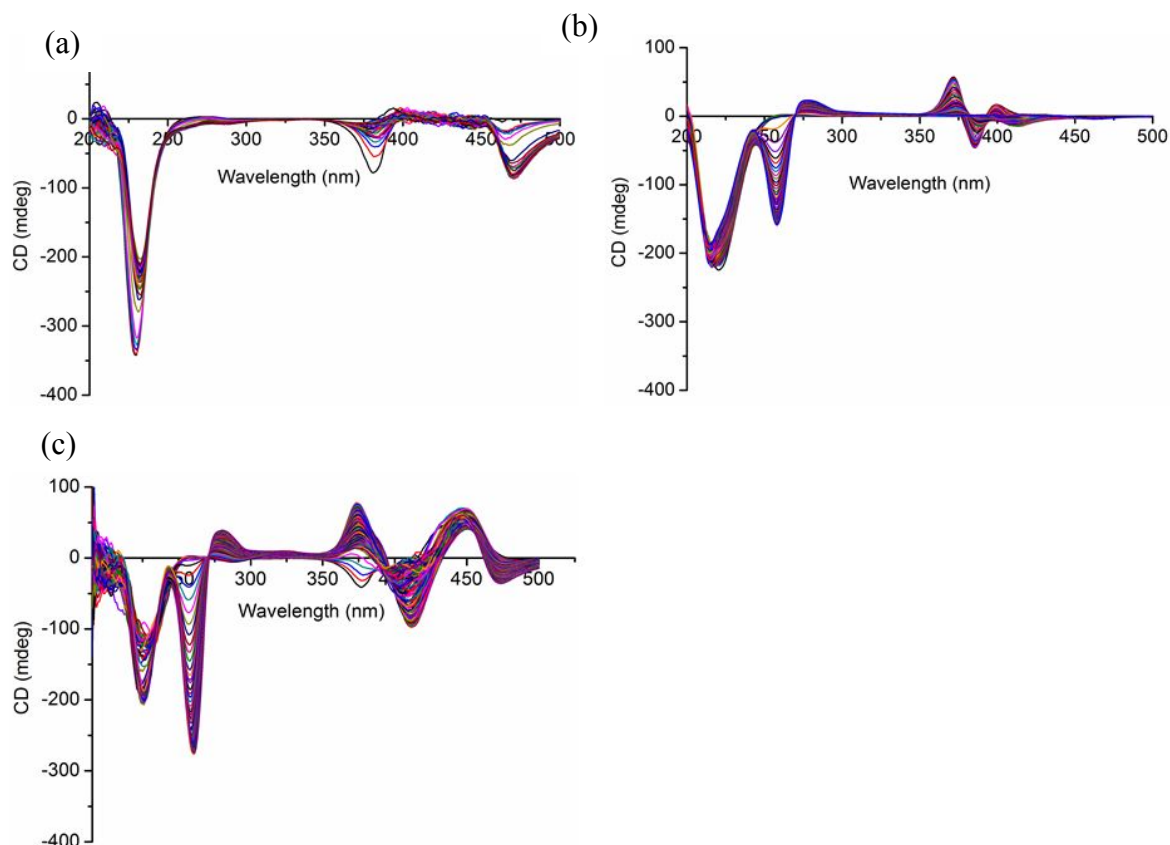


**Figure S3.** Circular dichroism spectra confirming that ThT was incorporated into nanofibers of (a) **PA-E3**, (b) **DBS-COOH** and (c) their equimolar in a differential and time-dependent manner. The band at 218 nm is a circular dichroic signature of gluconic acid which results from the base-catalysed hydrolysis of GdL. It is also expected that **PA-E3** should display the

characteristic  $\beta$ -sheet signature of peptide amphiphiles at this region. In (b), DBS-COOH exhibits a strong negative absorption at 254 nm (due to the chiral sugar backbone) and a weak positive signal at 280 nm (due to the aromatic chromophores). ThT exhibit different CD signatures depending on the chiral environment.

## 5. TEM characterization of nanostructures of PA-E3, DBS-COOH and their co-assemblies

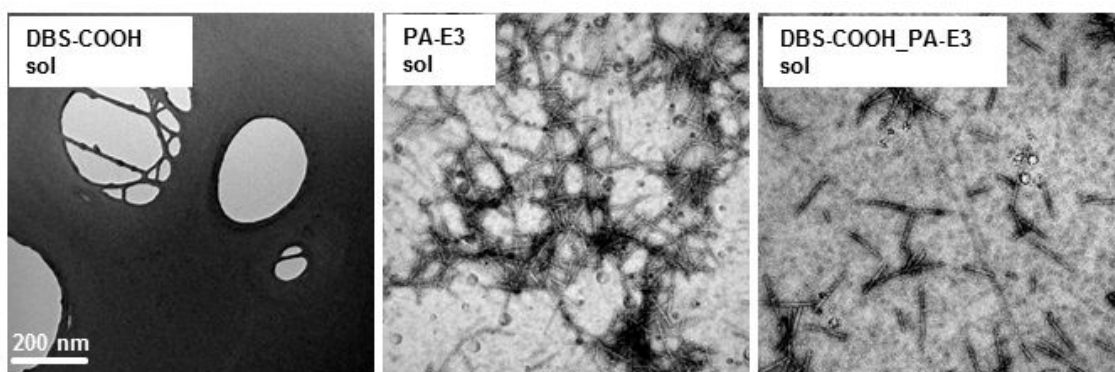


**Figure S4.** TEM images showing the pre-gelation nanostructures of **PA-E3** alone sol and in **PA-E3/DBS-COOH** admixtures against **DBS-COOH** alone sol.

## 6. Small-Angle Neutron Scattering (SANS) analysis of hydrogel nanostructures

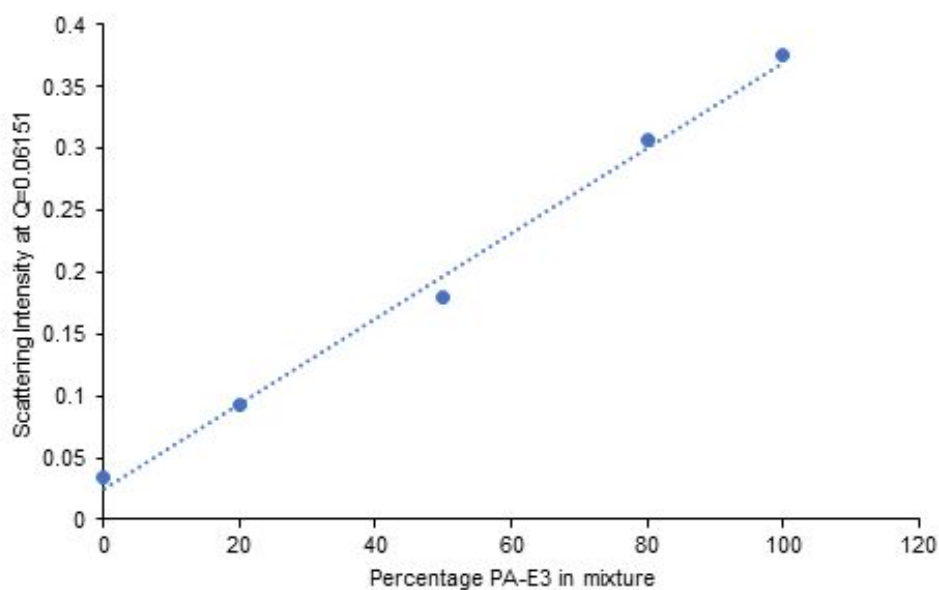


**Figure S5.** A plot of intensity at Q of 0.06151 against % **PA-E3** in the mixture.

**Table S1.** Summary of SANS data fitting parameters (\* represents an arbitrary number)

	<b>PA-E3</b>	<b>PA-E3/DBS-COOH (4:1)</b>	<b>PA-E3/DBS-COOH (1:1)</b>	<b>PA-E3/DBS-COOH (1:4)</b>	<b>DBS-COOH</b>
SLD (estimated) / $\times 10^{-6} \text{ \AA}^{-2}$	1.310	1.4874	1.7535	2.0196	2.197
Background / $\text{cm}^{-1}$	$0.021 \pm 0.0002$	$0.013 \pm 0.0002$	$0.014 \pm 0.0002$	$0.016 \pm 0.000$	$0.0129 \pm 0.0001$
Axis ratio	$1.637 \pm 0.015$	$1.53 \pm 0.03$	$1.360 \pm 0.06$	$1.524 \pm 0.10$	
Kuhn Length / $\text{Å}$	$134.0 \pm 2.0$	$111.6 \pm 2.1$	$96.3 \pm 3.15$	$114.4 \pm 9.21$	
Length / $\text{Å}$	2000*	2000*	2000*	2000*	
Radius / $\text{Å}$	$26.9 \pm 0.1$	$27.5 \pm 0.3$	$28.4 \pm 0.7$	$27.9 \pm 1.1$	
Scale (flex ellip cyl)	$1.62 \times 10^{-3} \pm$ $1.155 \times 10^{-5}$	$1.377 \times 10^{-3} \pm$ $1.4096 \times 10^{-5}$	$8.264 \times 10^{-3} \pm$ $2.440 \times 10^{-6}$	$3.962 \times 10^{-4} \pm$ $1.582 \times 10^{-5}$	
Power Law		$2.47 \pm 0.05$	$2.76 \pm 0.04$	$2.947 \pm 0.07$	$2.716 \pm 0.009$
Scale (power law)		$2.054 \times 10^{-5} \pm$ $5.287 \times 10^{-6}$	$1.303 \times 10^{-5} \pm$ $2.825 \times 10^{-6}$	$5.089 \times 10^{-6} \pm$ $1.779 \times 10^{-6}$	$1.183 \times 10^{-5} \pm$ $4.185 \times 10^{-7}$
$\chi^2$	5.936	5.4074	8.5144	2.888	4.6165

## 7. Rheological kinetics for PA-E3, DBS-COOH and PA-E3/DBS-COOH equimolar mixture

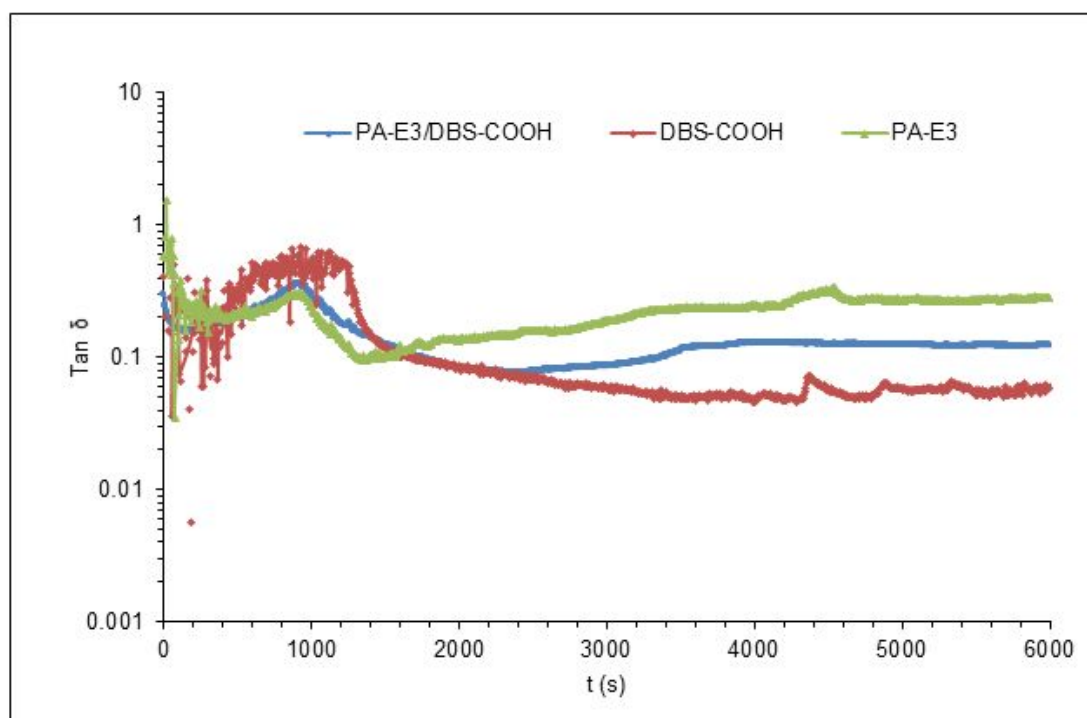


**Figure S6.** Time-sweep rheology showing variation of  $\tan \delta$  with time as an evidence of sol-gel phase transition.

## 8. Avrami Equation

By fitting the data acquired through dynamic time sweep rheology into an Avrami model (eq 1 - 4), we were able to gain further insight into the dimensionality of the nanoscale assembly. This model has been applied previously to study the growth kinetics of molecular gelators. The  $X(t)$  represents the volume fraction of the self-assembled (gel) phase, the temperature-dependent constant  $K$  (similar to a rate constant), and the Avrami exponent  $n$  represents the type of growth leading to phase separation.

$$1 - X(t) = \exp(-Kt^n) \quad (1)$$

$$\ln(\ln(1/(1 - X(t)))) = \ln K + n \ln(t) \quad (2)$$

$$X(t) = (I(\infty) - I(t)) / (I(\infty) - I(0)) \quad (3)$$

$X(t)$  can be expressed in terms of the experimental values such as  $G'$  values at equilibrium ( $G'(\infty)$ ), at time  $t$  ( $G'(t)$ ) and at the start of the measurement ( $G'(0)$ ). Therefore,

$$G'(t) = (G'(\infty) - G'(t)) / (G'(\infty) - G'(0)) \quad (4)$$

Linear fitting of equation 2 into equation 4 enables the determination of the Avrami exponent  $n$ .

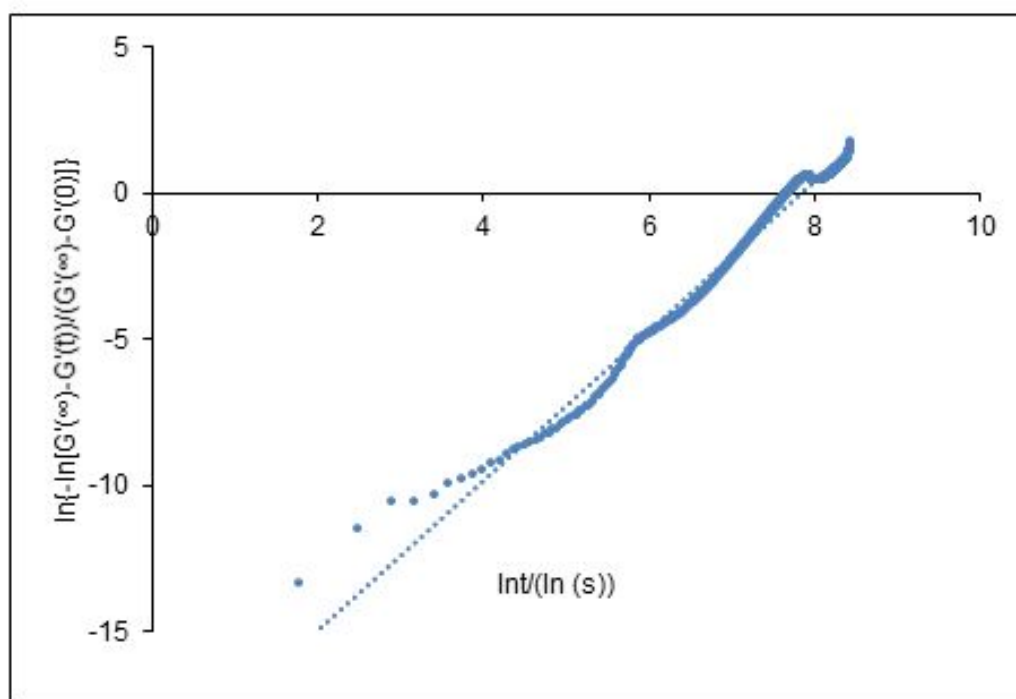


**Figure S7.** Plots of  $G'$  values according to Avrami model for sol-hydrogel phase transition of 10 mM of equimolar mixture of **PA-E3/DBS-COOH** (slope = 2.7,  $R^2 = 0.983$ ).

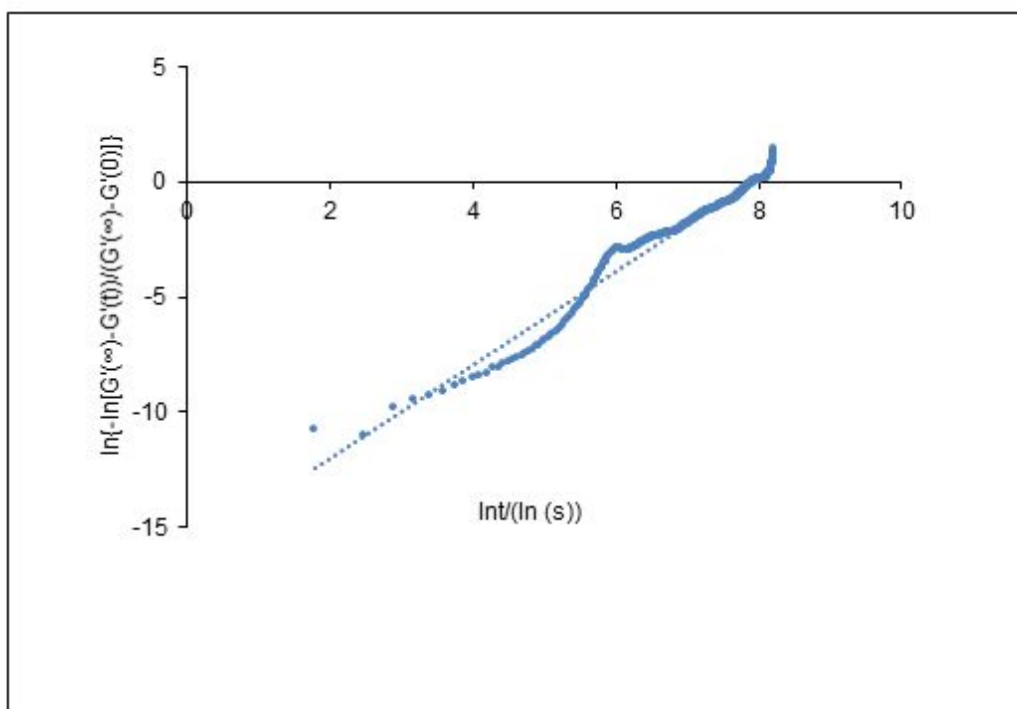


**Figure S8.** Plots of  $G'$  values according to Avrami model for sol-hydrogel phase transition of 10 mM of **PA-E3** (slope = 2.0,  $R^2 = 0.974$ ).

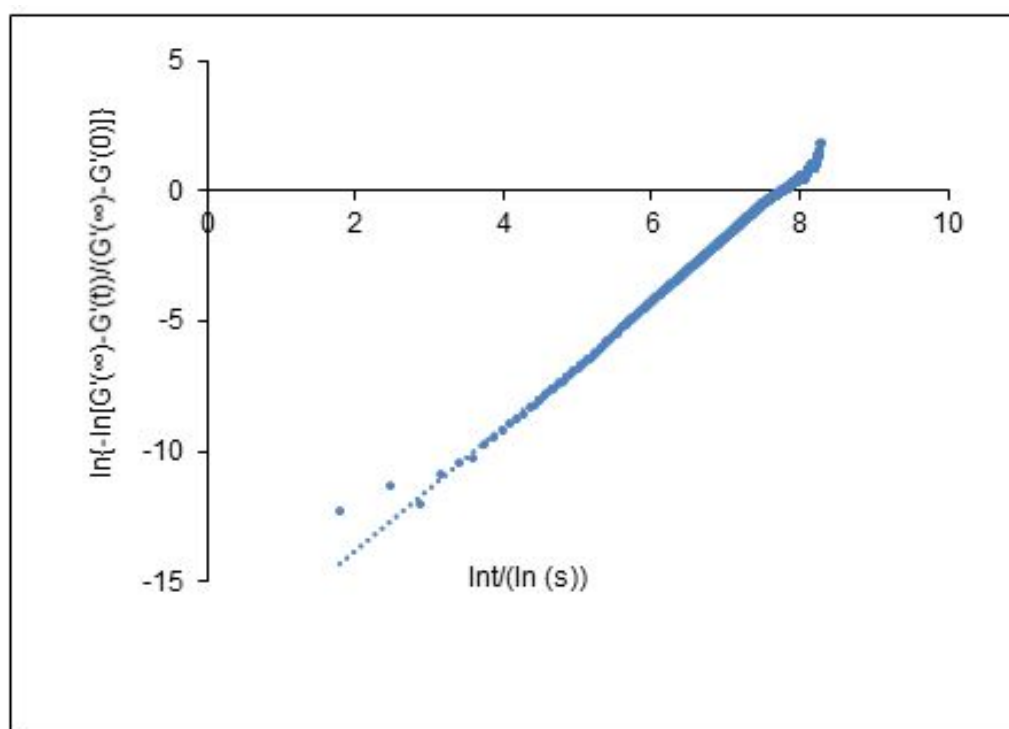


**Figure S9.** Plots of  $G'$  values according to Avrami model for sol-hydrogel phase transition of 10 mM of **DBS-COOH** (slope = 2.2,  $R^2 = 0.996$ ).



## 9. Molecular dynamic simulation details

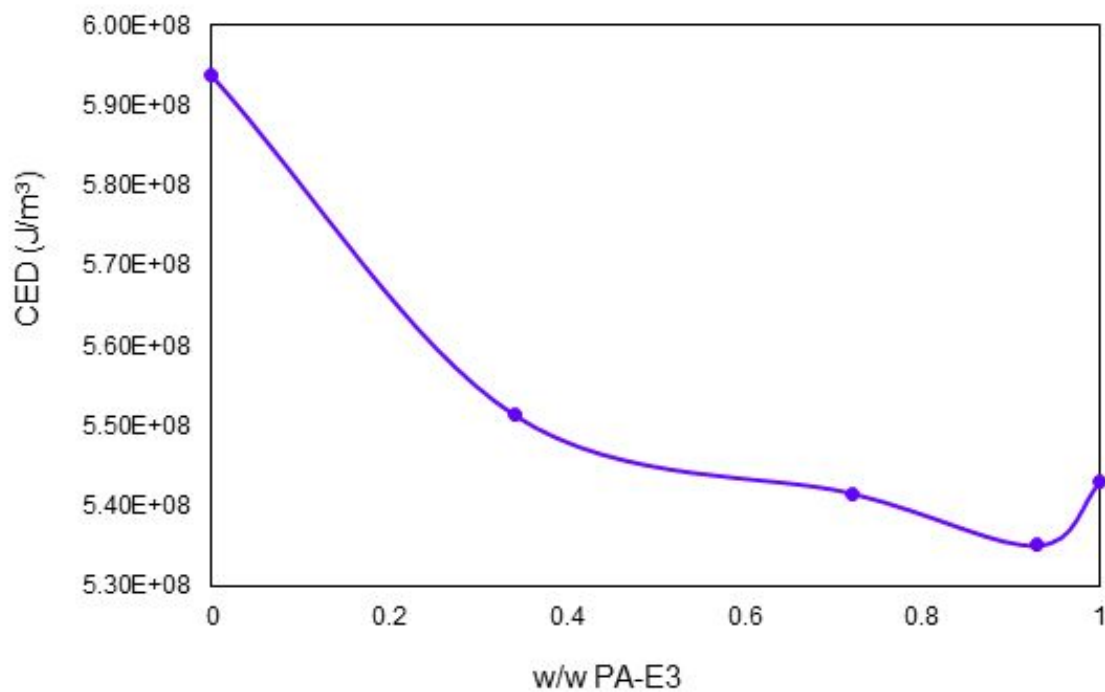


**Figure S10.** Cohesive energy density (CED) of PA-E3 and DBS-COOH blends

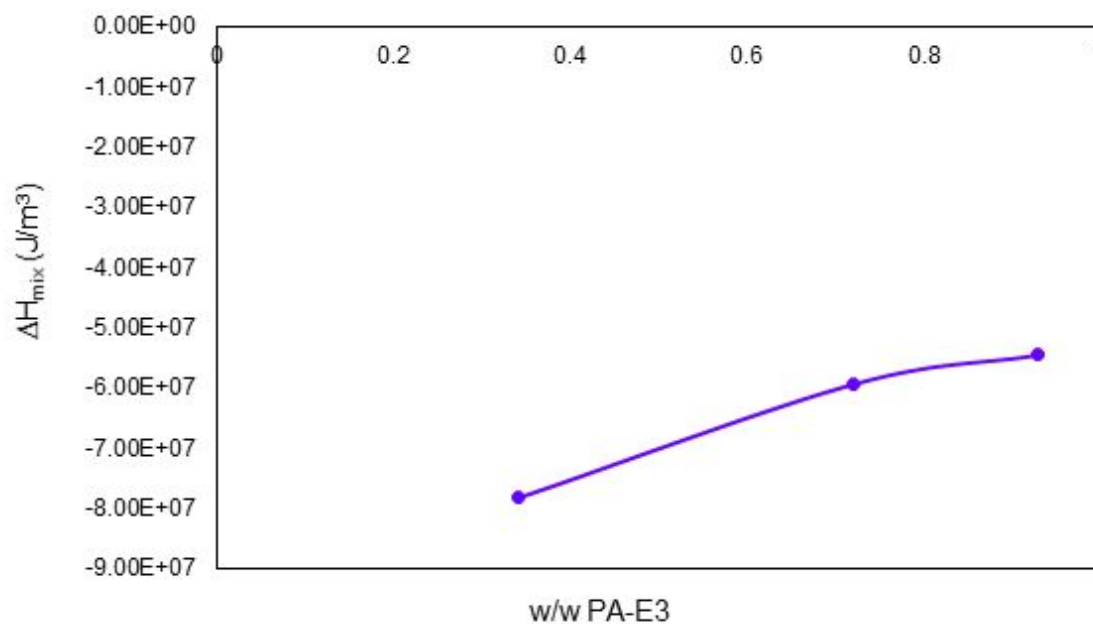


**Figure S11.** Enthalpy of mixing ( $\Delta H_{\text{mix}}$ ) of PA-E3 and DBS-COOH blends.

**Table S2.** Summary of intermolecular interaction distances between **PA-E3, DBS-COOH** and their co-assemblies.

Interaction between	Interaction distance (Å)
O_carbonyl of DBSCOOH and H-amide of E3	1.58
O_carbonyl of DBSCOOH and H_carboxyl of E3	1.73
O5 of DBSCOOH and H-amide of E3	2.10
O6 of DBSCOOH and H-amide of E3	2.00

**10. Amplitude sweeps, critical strain and self-recovery of hydrogels**

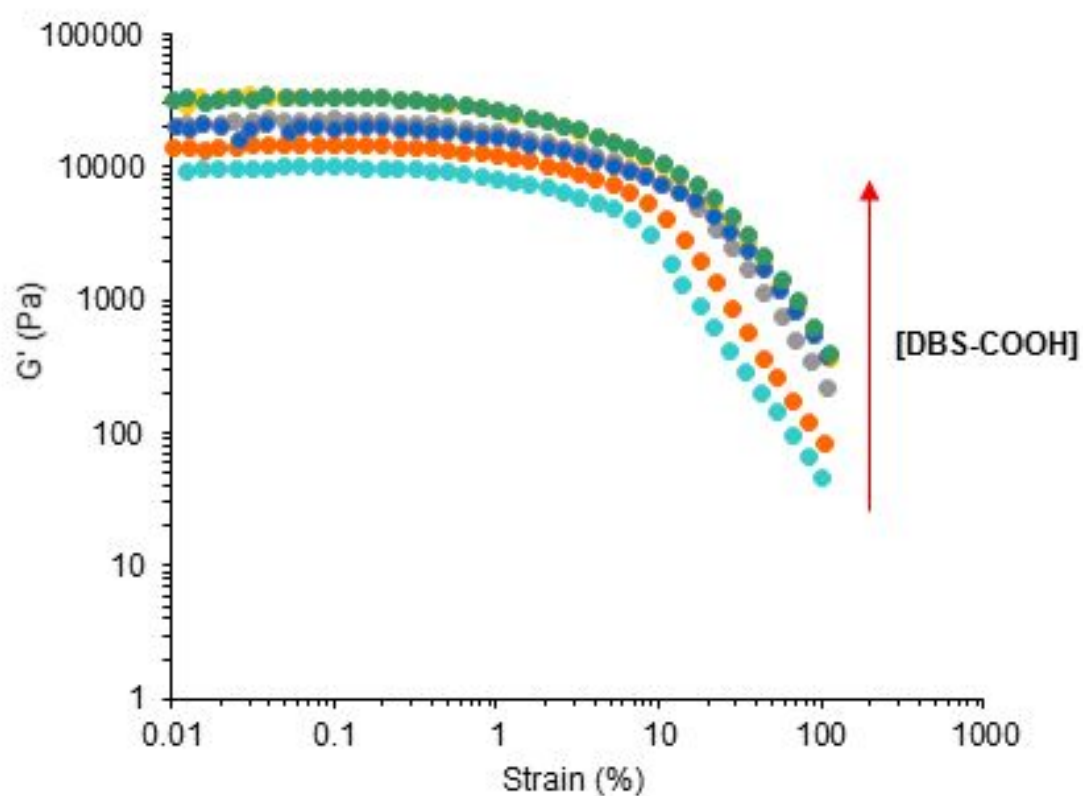


**Figure S12.** Amplitude sweep rheographs showing increasing storage modulus with concentration of **DBS-COOH**.

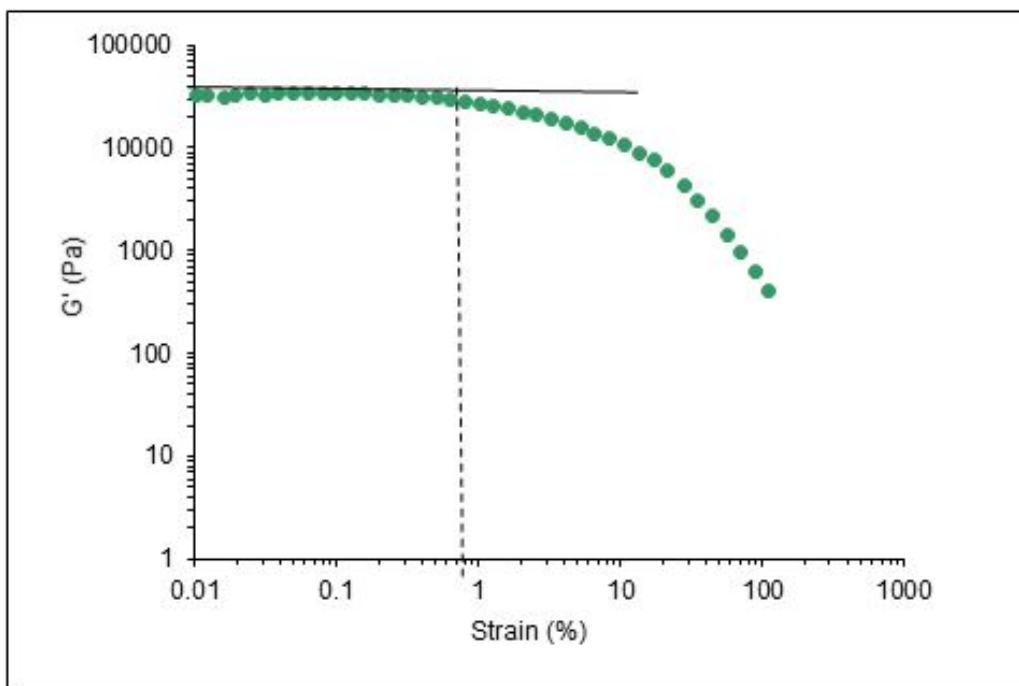


**Figure S13.** Critical strain of pure **DBS-COOH** hydrogel.

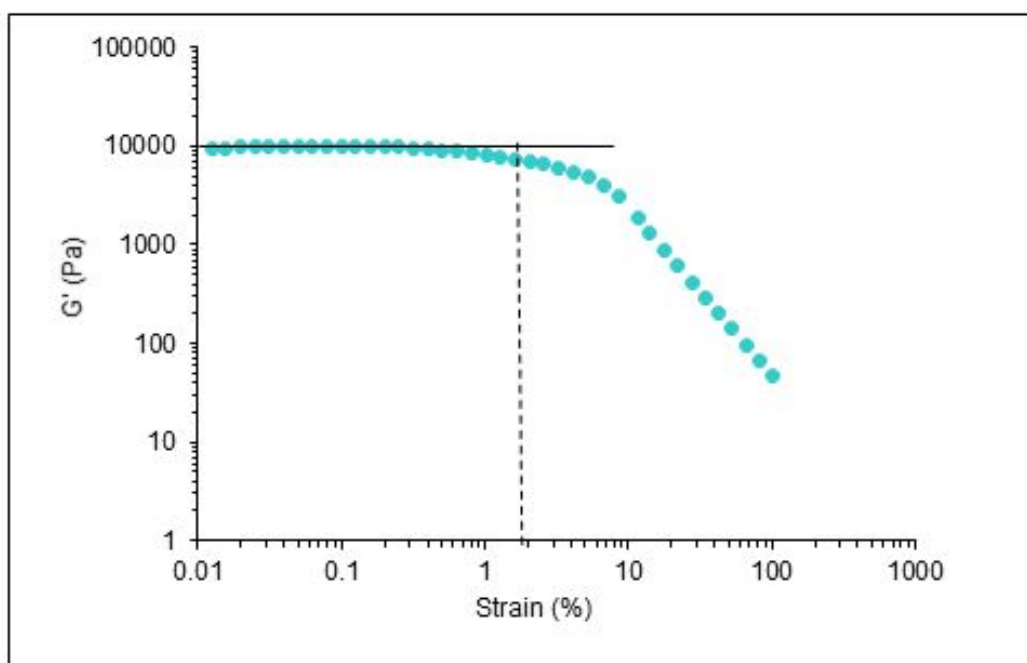


**Figure S14.** Critical strain of pure **PA-E3** hydrogel.

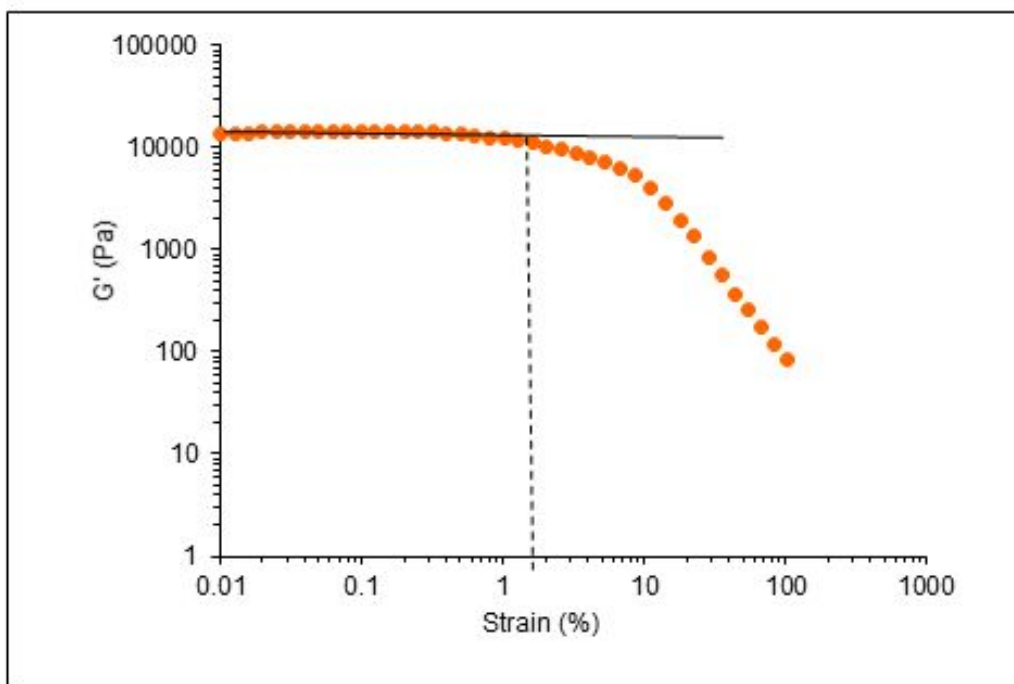


**Figure S15.** Critical strain of 80% **PA-E3** + 20% **DBS-COOH** hydrogel.

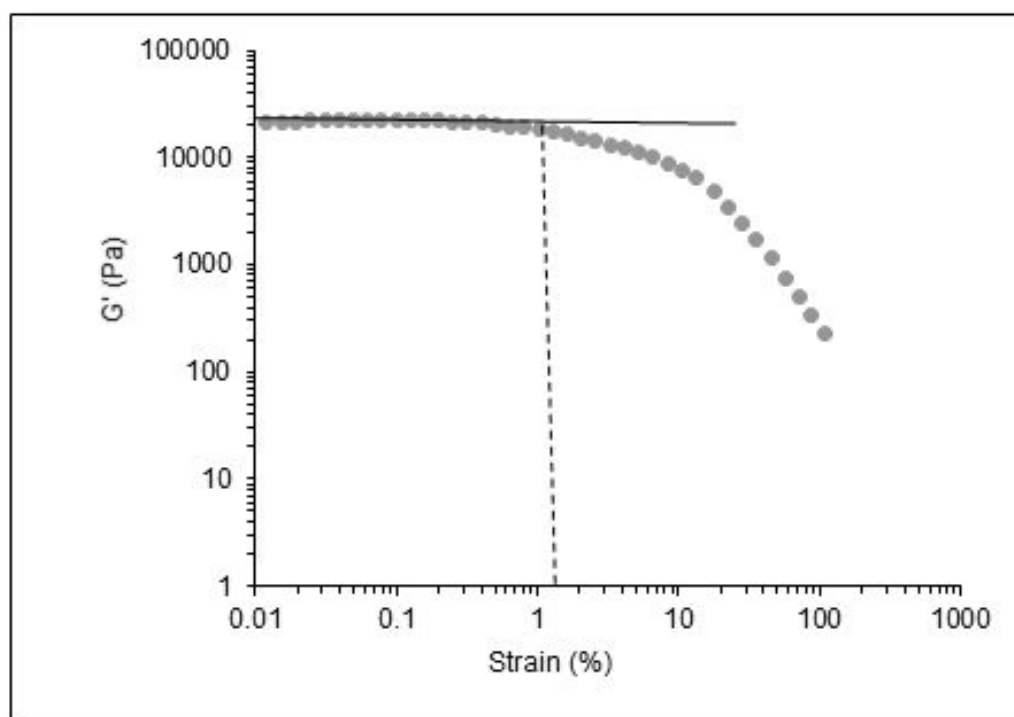


**Figure S16.** Critical strain of 60% **PA-E3** + 40% **DBS-COOH** hydrogel.

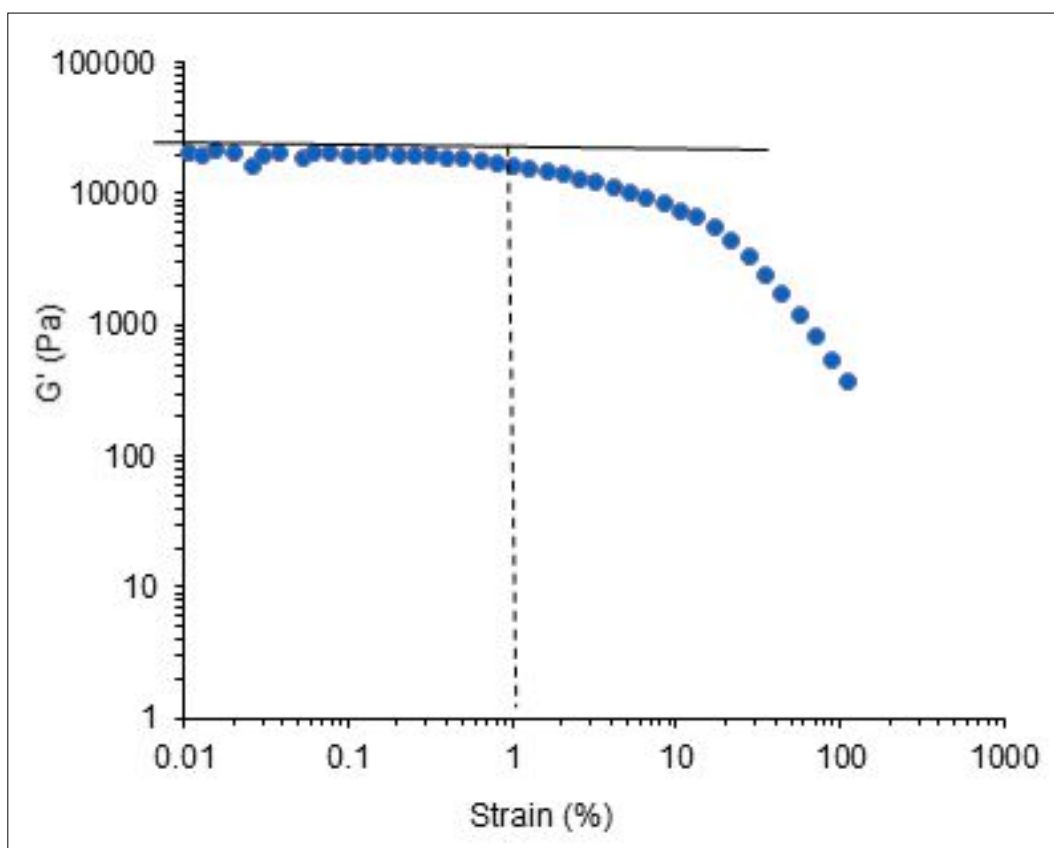


**Figure S17.** Critical strain of 40% PA-E3 + 60% DBS-COOH hydrogel.

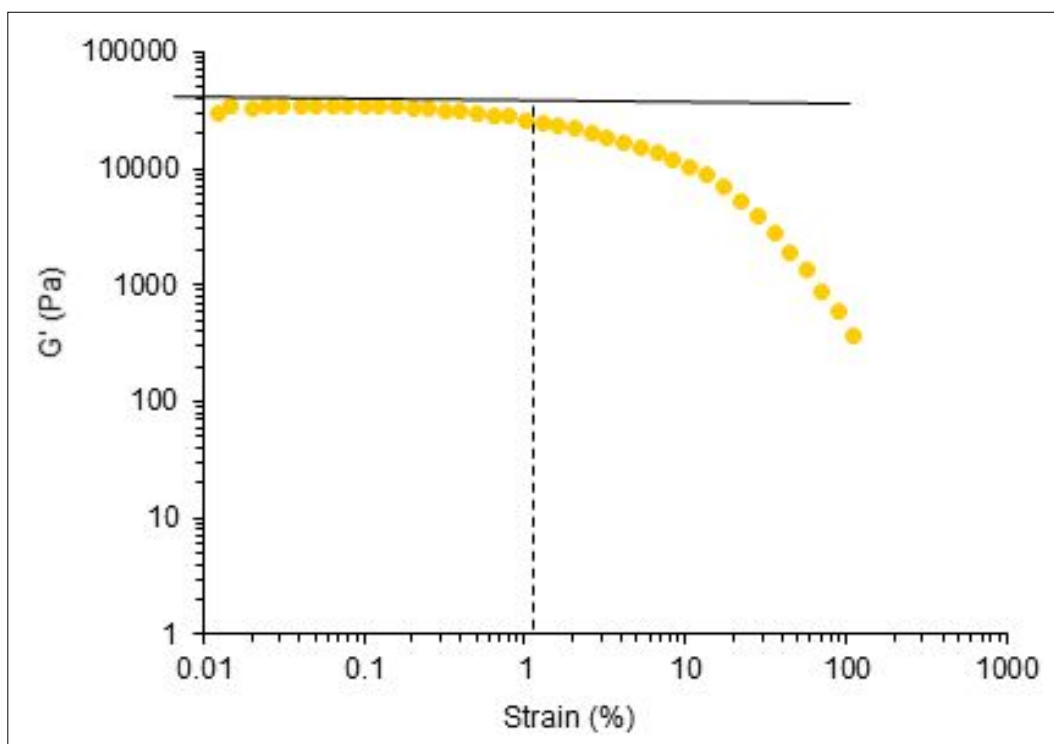


**Figure S18.** Critical strain of 20% PA-E3 + 80% DBS-COOH hydrogel.

## 11. Characterizing proteolytic stability of the hydrogels with mass spectrometry

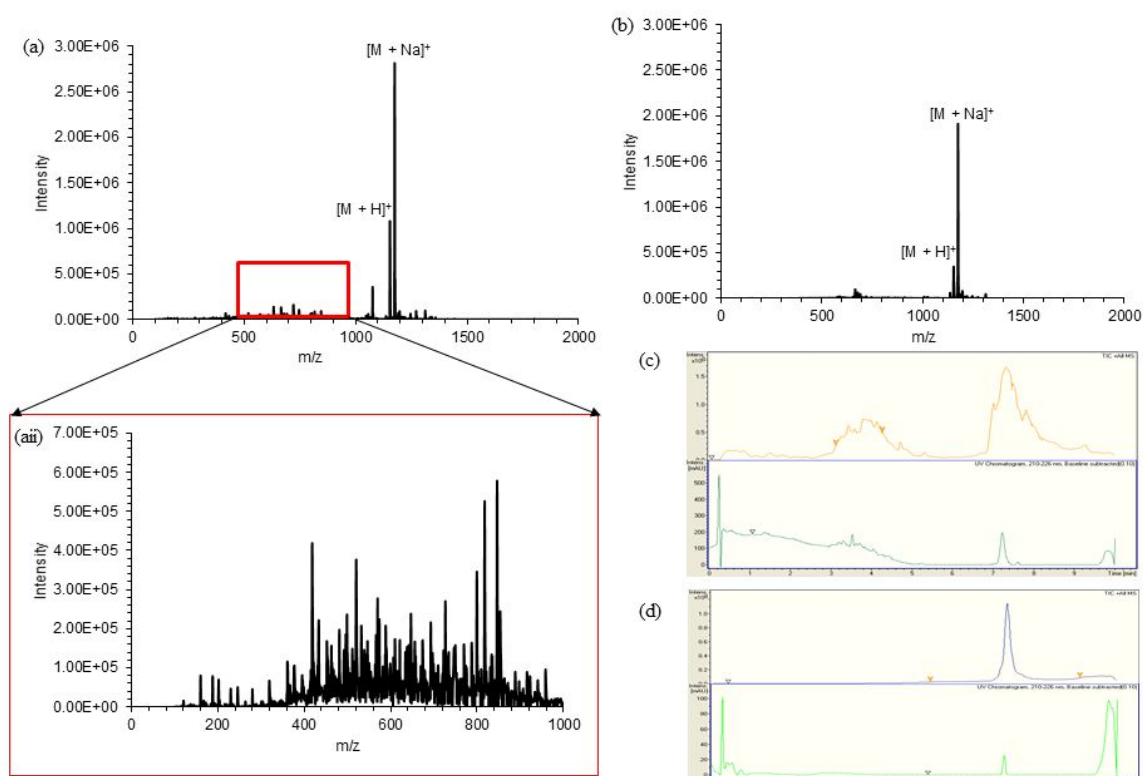


**Figure S19.** LC-MS for a mixture of (a and aii) 0.1 mM PA-E3/proteinase K (5 mg/mL), (b) 0.1 mM PA-E3/0.1 mM DBS-COOH/proteinase K (5 mg/mL), (c) TIC and UV trace for 0.1 mM PA-E3/proteinase K (5 mg/mL) and (d) 0.1 mM PA-E3/0.1 mM DBS-COOH/proteinase K (5 mg/mL).

## References

- (1) Mata, A.; Palmer, L.; Tejeda-Montes, E.; Stupp, S. I. In *Nanotechnology in Regenerative Medicine: Methods and Protocols*; Navarro, M.; Planell, J. A., Eds.; Humana Press: Totowa, NJ, 2012, DOI:10.1007/978-1-61779-388-2\_3 10.1007/978-1-61779-388-2, pp. 39-49.
- (2) Cornwell, D. J.; Okesola, B. O.; Smith, D. K. Hybrid polymer and low molecular weight gels – dynamic two-component soft materials with both responsive and robust nanoscale networks. *Soft Matter* 2013, **9**, 8730-8736.